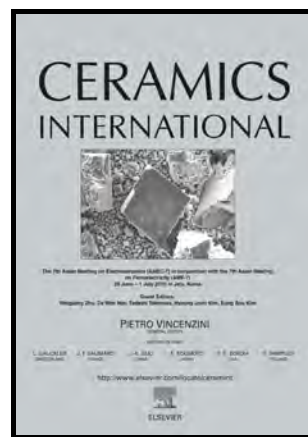


Phase transition and low-temperature sintering of
 $\text{Zn}(\text{Mn}_{1-x}\text{Al}_x)_2\text{O}_4$ ceramics for LTCC applications

Xue-Kai Lan, Zheng-Yu Zou, Wen-Zhong Lu,
Jian-Hua Zhu, Wen Lei



www.elsevier.com/locate/ceri

PII: S0272-8842(16)31407-9
DOI: <http://dx.doi.org/10.1016/j.ceramint.2016.08.098>
Reference: CERI13550

To appear in: *Ceramics International*

Received date: 12 July 2016
Revised date: 27 July 2016
Accepted date: 16 August 2016

Cite this article as: Xue-Kai Lan, Zheng-Yu Zou, Wen-Zhong Lu, Jian-Hua Zhu and Wen Lei, Phase transition and low-temperature sintering of $\text{Zn}(\text{Mn}_{1-x}\text{Al}_x)_2\text{O}_4$ ceramics for LTCC applications, *Ceramics International*, <http://dx.doi.org/10.1016/j.ceramint.2016.08.098>

This is a PDF file of an unedited manuscript that has been accepted for publication. As a service to our customers we are providing this early version of the manuscript. The manuscript will undergo copyediting, typesetting, and review of the resulting galley proof before it is published in its final citable form. Please note that during the production process errors may be discovered which could affect the content, and all legal disclaimers that apply to the journal pertain.

Phase transition and low-temperature sintering of $\text{Zn}(\text{Mn}_{1-x}\text{Al}_x)_2\text{O}_4$ ceramics for LTCC applications

Xue-Kai Lan^{a,b}, Zheng-Yu Zou^{a,b}, Wen-Zhong Lu^{a,b}, Jian-Hua Zhu^c, Wen Lei^{a,b*}

^aSchool of Optical and Electronic Information, Huazhong University of Science and Technology, Wuhan 430074, P. R. China

^bKey Lab of Functional Materials for Electronic Information (B), Ministry of Education, Wuhan 430074, P. R. China

^cShen Zhen Zhen Hua Ferrite & Ceramic Electronics Co., Ltd., Shenzhen 518109, P.R. China

* Corresponding author. Tel.: +86 27 8755 6493; fax: +86 27 8754 3134. *E-mail address:* wenlei@mail.hust.edu.cn (W. Lei)

Abstract

The phase transition, sinterability, and microwave dielectric properties of $\text{Zn}(\text{Mn}_{1-x}\text{Al}_x)_2\text{O}_4$ ($0.2 \leq x \leq 0.9$) solid solutions synthesized through a solid-state reaction were investigated. The densification temperature of the solid solutions decreased to 1250 °C, which is much lower than that of the end members. All compositions showed a single phase with a tetragonal structure at $x \leq 0.6$ and a cubic structure at $0.7 \leq x \leq 0.9$. As the x value increased, the ε_r value decreased gradually along with an inflection point of a sharp drop at $x=0.7$. The $Q \times f$ value significantly increased initially and reached the maximum value of 14460 GHz at $x=0.8$; it decreased

thereafter. Meanwhile, the τ_f value was near the typical value of about -60 ppm/ $^{\circ}\text{C}$ to -80 ppm/ $^{\circ}\text{C}$. TiO_2 and $\text{ZnO-B}_2\text{O}_3$ (ZB) glass co-doping can effectively adjust the τ_f value of $\text{Zn}(\text{Mn}_{0.2}\text{Al}_{0.8})_2\text{O}_4$ composition, with the highest $Q \times f$ value near zero, and can reduce its sintering temperature to 950 $^{\circ}\text{C}$. The $(1-y)\text{Zn}(\text{Mn}_{0.2}\text{Al}_{0.8})_2\text{O}_4-y\text{TiO}_2$ ($y=0.26$) ceramics with 5 wt.% ZB glass exhibited microwave dielectric properties ($\epsilon_r=12.71$, $Q \times f=8126$ GHz, and $\tau_f=1.02$ ppm/ $^{\circ}\text{C}$) appropriate for application in low-temperature co-fired ceramics (LTCC).

Keywords:

$\text{Zn}(\text{Mn}_{1-x}\text{Al}_x)_2\text{O}_4$; Dielectric ceramics; Phase transition; LTCC

1. Introduction

Recent developments in modern microwave communication technologies have resulted in a great demand for substrate materials with very low relative permittivity ($\epsilon_r < 15$) [1]. A low ϵ_r value is generally harmful to the miniaturization of electronic components according to the following equation.

$$\lambda = \frac{\lambda_0}{\sqrt{\epsilon_r}} \quad (1)$$

where λ_0 and λ are wavelength in a vacuum and dielectrics with ϵ_r value, respectively. However, size reduction is unnecessary when the components are applied at millimeter-wave frequency because the size is in the order of millimeters. A low ϵ_r value has two advantages. The first is reduced time delay of the signal (T_{PD})

according to the following equation [2].

$$T_{PD} = \frac{\sqrt{\varepsilon_r}}{c} \quad (2)$$

where ε_r is the relative permittivity and c is the velocity of light. The second is the reduction of inductive crosstalk and noise generation [1]. Low dielectric loss ($\tan\delta$) is another critical requirement to increase selectivity and reduce energy consumption. This property is characterized by the quality factor ($Q \times f$, $Q=1/\tan\delta$, and f is resonant frequency). Moreover, a near-zero temperature coefficient of resonant frequency (τ_f) is also required to ensure the stability of the frequency against temperature change [3].

Small, lightweight, multifunctional electronic components are currently attracting much attention in actual applications. Thus, manufacturers are forced to search for new advanced integration, packaging, and interconnection technologies. A solution to this problem is low-temperature co-fired ceramic (LTCC) technology [3] that enables the fabrication of 3D ceramic modules with a low dielectric loss and embedded silver electrodes. The $Q \times f$ value of LTCC materials is not less than 1000 GHz and is generally lower than that of resonator materials because the main losses originate from the conductor rather than dielectrics [4].

Recently, Cao et al. [5, 6] reported that the phase compositions and microwave dielectric properties of zinc manganese ceramics sintered at 1450 °C in air are subjected to the effects of different Zn/Mn ratios. When the Zn/Mn ratio was less than 1/3, a single ZnMn_2O_4 -based spinel-like phase was observed and exhibited low-permittivity microwave dielectric properties. For example, typical values (ε_r ,

$=7.32$, $Q \times f = 13667$ GHz, and $\tau_f = -58.33$ ppm/°C) were obtained for the nominal ZnMn_3O_7 ceramic with a $(\text{Zn,Mn})\text{Mn}_2\text{O}_4$ structure. However, the nominal ZnMn_2O_4 ceramic sintered at 1450 °C for 3 h in air did not possess microwave dielectric properties because an excess ZnO second phase with a large dielectric loss existed in the core-shell reaction model [6].

Although the ZnAl_2O_4 system has higher sintering temperature (1650 °C) [7], it exhibits a similar lattice structure and much higher $Q \times f$ value ($Q \times f = 106000$ GHz), compared with ZnMn_2O_4 . Thus, the $Q \times f$ value of ZnMn_2O_4 ceramics can be improved by partial substitution of Al^{3+} for Mn^{3+} cations. Interestingly, partial substitution strengthens ion diffusion to form a single phase, reduces the sintering temperature to 1250 °C, and provides the $\text{Zn}(\text{Mn}_{1-x}\text{Al}_x)_2\text{O}_4$ system good microwave dielectric properties. To meet the requirements of LTCC applications, low-melting-point oxides or glass, such as $\text{ZnO-B}_2\text{O}_3$ (ZB) [8-10], B_2O_3 [11], $\text{Li}_2\text{O-ZnO-B}_2\text{O}_3$ (LZB) [12], $\text{ZnO-SiO}_2\text{-B}_2\text{O}_3$ (ZSB) [13], and $\text{BaO-SiO}_2\text{-B}_2\text{O}_3$ (BSB) [14], are frequently utilized as sintering aids. In the $\text{ZnO-MnO}_2\text{-TiO}_2$ system, Cao et al. [5] found that ZB glass not only effectively reduces the sintering temperature to 950 °C but also retains good microwave dielectric properties.

Therefore, the sinterability, phase transition, and microwave dielectric properties of $\text{Zn}(\text{Mn}_{1-x}\text{Al}_x)_2\text{O}_4$ ceramics were investigated in this study. The effects of ZB glass as a sintering aid and TiO_2 as τ_f compensator on the low-temperature sintering characteristics and microwave dielectric properties of $\text{Zn}(\text{Mn}_{1-x}\text{Al}_x)_2\text{O}_4$ ($x=0.8$) ceramics with the highest $Q \times f$ value were also examined through LTCC application.

2. Experimental procedure

$\text{Zn}(\text{Mn}_{1-x}\text{Al}_x)_2\text{O}_4$ ($x=0.2, 0.4, 0.5, 0.6, 0.7, 0.8, 0.9$) ceramics were prepared by a solid-state reaction process, where the reagent-grade ZnO , Al_2O_3 , and MnO_2 powders were used as the raw materials. The weighed raw materials were mixed by ball milling with zirconia media in alcohol for 5 h, and the mixtures were calcined at $1100\text{ }^\circ\text{C}$ in air for 3 h after drying. The calcined powders were pressed into disks with 12 mm in diameter and about 6 mm in height, and then sintered at $1250\text{ }^\circ\text{C}$ in air for 3 h. These samples were cooled at a rate of $1\text{ }^\circ\text{C}/\text{min}$ down to $1000\text{ }^\circ\text{C}$, then at a rate of $2\text{ }^\circ\text{C}/\text{min}$ down to $800\text{ }^\circ\text{C}$, and finally furnace cooled.

The ZB glass was prepared using the mixed glass method. The reagent-grade ZnO and H_3BO_3 (raw materials) were mixed in a molar ratio of 1:2. The mixture was then fused in an alumina crucible at $1100\text{ }^\circ\text{C}$ for 2 h, and the molten glass was poured into cold water for quenching. The glass frit was roughly crushed in an aluminum mortar and then planetary-milled in a deionized water medium for 3 h. After being dried and sieved, the glass frit powder was as prepared.

For the ZB glass and TiO_2 containing samples, 5 wt.%ZB glass was added to the calcined $(1-y)\text{Zn}(\text{Mn}_{0.2}\text{Al}_{0.8})_2\text{O}_4-y\text{TiO}_2$ powders, and then were re-milled together for 5 h. Following the same drying and forming procedures, the pellets were sintered at $950\text{ }^\circ\text{C}$.

The polycrystalline phases were identified by X-ray diffraction using an automated diffractometer (XRD-7000, Shimadzu Corporation, Japan) equipped with a crystal monochromator employing $\text{CuK}\alpha$ radiation. In addition, the lattice parameters

were obtained by Rietveld refinement using the GSAS software [15, 16]. The microstructure was observed by scanning electron microscope (SEM, Sirion 200, Netherlands). The ε_r and unloaded $Q \times f$ value was measured in the TE₀₁₁ mode at about 12 GHz by the Hakki and Coleman method [17] using a microwave network analyzer (Agilent E8362B, Agilent Technologies, USA) and two parallel silver boards. The τ_f value in the temperature range of 30–80 °C was calculated by formula (3):

$$\tau_f = \frac{1}{f(T_0)} \frac{[f(T_1) - f(T_0)]}{T_1 - T_0} \quad (3)$$

where $f(T_1)$ and $f(T_0)$ represent the resonant frequency at T_1 (80 °C) and T_0 (30 °C), respectively. Impedance analysis of pellets coated Ag electrode was performed over the frequency range from 100 Hz to 10 MHz, using an impedance analyzer (Agilent 4294A, Agilent Technologies, USA). And all data were corrected for sample geometry and analyzed using in-house software.

3. Results and discussion

The X-ray diffraction (XRD) patterns of the Zn(Mn_{1-x}Al_x)₂O₄ ceramics sintered at 1250 °C for 3 h are shown in Fig. 1. For Zn(Mn_{1-x}Al_x)₂O₄ ceramics with a composition range of 0.2 ≤ x ≤ 0.6, the XRD profiles show the presence of a tetragonal phase. The samples obtained at a composition range of 0.7 ≤ x ≤ 0.9 show a cubic solid solution phase. This result suggests that phase transition in the solid solutions occurred at approximately $x=0.7$.

As the x value increased from 0.2 to 0.6, lattice symmetry improved gradually, as shown in Fig. 1. The diffraction peaks of the Zn(Mn_{1-x}Al_x)₂O₄ ($x = 0.7, 0.8, 0.9$) solid

solution shifted to a high angle of 2θ with the increase in the x value. This result indicates that shrinkage of lattice volume occurred because the ion radii of Mn^{3+} and Al^{3+} were 0.645 and 0.535 Å, respectively.

Fig. 2 presents the lattice parameters of the $\text{Zn}(\text{Mn}_{1-x}\text{Al}_x)_2\text{O}_4$ solid solution as a function of the x value. The lattice parameters c of the tetragonal structure decreased linearly and parameter a increased slightly when x ranged from 0.2 to 0.6. With the further increase in the x value, the compound transformed from a tetragonal to a cubic structure, and parameter a decreased slightly because of the increase in Al^{3+} substitution for the Mn^{3+} site.

The surface morphologies of the $\text{Zn}(\text{Mn}_{1-x}\text{Al}_x)_2\text{O}_4$ ($x=0.4-0.9$) ceramics sintered at 1250 °C for 3 h in air were observed through scanning electron microscopy (SEM), and the results are shown in Fig. 3. The glass phase was observed in the ceramics with a small amount of Al^{3+} . This finding indicates that the partial substitution of Al^{3+} for Mn^{3+} ions in $\text{Zn}(\text{Mn}_{1-x}\text{Al}_x)_2\text{O}_4$ was beneficial to the reduction of the sintering temperature and prompted densification because pure ZnMn_2O_4 ceramics cannot be sintered well until 1450 °C and exhibit porous microstructures [6, 18]. However, the grain size decreased gradually with the increase in the x value, which could be a result of the reduction in the glass phase. Generally, glass phase as a liquid phase during sintering helps improve ion diffusion and contributes to grain growth. As the x value increased to 0.9, the composition approached that of the high-temperature ZnAl_2O_4 phase, and the glass phase was almost not observed in Fig. 3(f). Therefore, it is rational to conclude that the smallest average grain size exists in the composition of

$x=0.9$.

The microwave dielectric properties of the $\text{Zn}(\text{Mn}_{1-x}\text{Al}_x)_2\text{O}_4$ ceramics sintered at 1250 °C in air for 3 h were then investigated. The microwave dielectric properties depended largely on the Al^{3+} content (x value). Fig. 4 shows the variation in relative permittivity (ϵ_r) of the sintered ceramics as a function of the x value. As the x value increased from 0.2 to 0.7, the ϵ_r value decreased slightly from 10.28 to 9.54. The ϵ_r value decreased significantly when the x value exceeded 0.7. This trend in ϵ_r value corresponds to the phase transition of the solid solutions that occurred at $x=0.7$ (see Figs. 2 and 4). The dielectric constant generally depends on density and ionic polarizability aside from the lattice structure. According to the Clausius–Mossotti equation, the dielectric constant depends on polarizability and the molar volume of the compounds. The reduction in the dielectric constant in this study can be well explained by the low dielectric polarizability of Al^{3+} ion in place of high polarizability of Mn^{3+} ; thus, the dielectric constant decreased monotonously as the Al^{3+} content increased. Fig. 3 shows that grain size decreased with the increase in the Al^{3+} content due to the reduce in glass phase, which could also induce a decrease in the dielectric constant.

Fig. 5 shows the $Q \times f$, τ_f , and relative density of the $\text{Zn}(\text{Mn}_{1-x}\text{Al}_x)_2\text{O}_4$ ceramics as a function of the x value. As the x value increased, the $Q \times f$ value (Fig. 5(a)) of the samples increased initially from 3144 GHz to 14460 GHz and then decreased after reaching the maximum value at $x=0.8$. The τ_f value changed only slightly from –60 ppm/°C to –80 ppm/°C (Fig. 5(b)), which is a typical value for low-permittivity

microwave dielectric ceramics on the basis of the ε_r - τ_f relationship [19]. And the relative density remained at about 95% when the x value was below 0.8. However, when $x=0.9$, the relative density decreased rapidly to approximately 85% (Fig. 5(c)), which corresponds to the variation trend of the $Q \times f$ value with Al^{3+} content.

Generally, lattice defects (vacancies and dislocations), second phase, porosity, band gap, glass phase, and other microstructure-related defects exerted a strong influence on the $Q \times f$ value [20–22]. In this study, the amount of Al^{3+} ions played an important role in improving the $Q \times f$ value of the $\text{Zn}(\text{Mn}_{1-x}\text{Al}_x)_2\text{O}_4$ ceramics because of the increase in the harmony between lattice vibration and the increase in the x value [23]. However, the decrease in the grain size (Fig. 3), especially the sharp drop of the relative density at $x=0.9$ (Fig. 5(c)), deteriorated greatly the $Q \times f$ value [24]. Thus, the two factors resulted in a maximum value at $x=0.8$ (Fig. 5(a)).

Fig. 6 presents an Arrhenius fitting plot of the temperature dependence of bulk conductivity (σ) for the $\text{Zn}(\text{Mn}_{1-x}\text{Al}_x)_2\text{O}_4$ ($0.2 \leq x \leq 0.9$) ceramics. As the x value increased, the activation energy (E_a) calculated from the slope of the fitting line increased from 0.48 eV to 0.54 eV. The approximation of the intrinsic band gap, $E_g \approx 2E_a$ [25, 26], indicated that conductivity decreased when the x value increased. Thus, the sample with a high x value had a better quality factor than the sample with a low x value.

To adjust the τ_f value to near zero and reduce the sintering temperature, TiO_2 and ZB glass were added to the $\text{Zn}(\text{Mn}_{1-x}\text{Al}_x)_2\text{O}_4$ ($x=0.8$) ceramics. Table 1 shows the microwave dielectric properties of $(1-y)\text{Zn}(\text{Mn}_{0.2}\text{Al}_{0.8})_2\text{O}_4 + y\text{TiO}_2$ with 5 wt.% ZB

glass sintered at 950 °C for 3 h. As the y value increased from 0.22 to 0.28, the τ_f value of the ceramics varied from -11.32 ppm/°C to 5.03 ppm/°C. This evidence indicates that ZB glass and TiO_2 co-doping in the $\text{Zn}(\text{Mn}_{0.2}\text{Al}_{0.8})_2\text{O}_4$ system not only reduced the sintering temperature by 300 °C but also effectively controlled the τ_f value to near zero. When the y value was equal to 0.26, the low-permittivity ceramics with an ε_r value of 12.71 exhibited a near-zero τ_f value ($\tau_f=1.02$ ppm/°C), although the $Q \times f$ value was not too high. In accordance with the requirement of the $Q \times f$ value for LTCC applications at microwave frequency, the value of 8027 GHz is higher than the value of 1000 GHz in the basic condition [4]. Therefore, $(1-y)\text{Zn}(\text{Mn}_{0.2}\text{Al}_{0.8})_2\text{O}_4+y\text{TiO}_2$ ($y=0.26$) ceramics with 5 wt.% ZB glass could be a promising candidate for LTCC components and modules.

4. Conclusions

- (1) $\text{Zn}(\text{Mn}_{1-x}\text{Al}_x)_2\text{O}_4$ ($0.2 \leq x \leq 0.9$) solid solutions were synthesized at 1250 °C for 3 h through solid-state reaction. The densification temperature was much lower than that of the end members. Phase transition from a tetragonal to a cubic structure occurred at $x=0.7$ with the increase in the x value.
- (2) As the x value increased from 0.2 to 0.7, the ε_r value decreased slightly from 10.28 to 9.54. The ε_r value decreased significantly when the x value exceeded 0.7. This trend in ε_r value corresponded to the phase transition of the solid solutions that occurred at $x=0.7$. The $Q \times f$ value increased initially from 3144 GHz to 14460 GHz and then decreased after reaching the maximum value at $x=0.8$. The τ_f value

changed only slightly near the typical value from $-60 \text{ ppm/}^\circ\text{C}$ to $-80 \text{ ppm/}^\circ\text{C}$.

- (3) ZB glass and TiO_2 co-doping in the $\text{Zn}(\text{Mn}_{0.2}\text{Al}_{0.8})_2\text{O}_4$ system not only decreased the sintering temperature by $300 \text{ }^\circ\text{C}$ but also effectively controlled the τ_f value to near zero. The $(1-y)\text{Zn}(\text{Mn}_{0.2}\text{Al}_{0.8})_2\text{O}_4+y\text{TiO}_2$ ($y=0.26$) ceramics with 5 wt.% ZB glass were sintered well at $950 \text{ }^\circ\text{C}$ for 3 h and exhibited appropriate microwave dielectric properties ($\epsilon_r=12.71$, $Q\times f=8126 \text{ GHz}$, and $\tau_f=1.02 \text{ ppm/}^\circ\text{C}$) for LTCC applications at microwave frequency.

Acknowledgements

This work was supported by the National Natural Science Foundation of China (NSFC-51572093) and the Fundamental Research Funds for the Central Universities (HUST-2015TS044). The authors are grateful to the Analytical and Testing Center, Huazhong University of Science and Technology, for SEM analyses.

References

- [1] Guo Y, Ohsato H, Kakimoto K, Characterization and dielectric behavior of willemite and TiO_2 -doped willemite ceramics at millimeter-wave frequency. *J. Eur. Ceram. Soc.* 2006, 26(10): 1827-1830.
- [2] Ohsato H, Tsunooka T, Sugiyama T, et al, Forsterite ceramics for millimeterwave dielectrics. *J. Electroceram.* 2006, 17(2-4): 445-450.
- [3] Fang L, Wei Z, Guo H, et al. Phase composition and microwave dielectric properties of low-firing $\text{Li}_2\text{A}_2\text{W}_3\text{O}_{12}$ (A=Mg, Zn) ceramics.

- J. Mater. Sci. - Mater. Electron. 2015, 26(8): 5892-5895.
- [4] Sebastian M T, Jantunen H, Low loss dielectric materials for LTCC applications: a review. *Int. Mater. Rev.* 2008, 53(2): 57-90.
- [5] Cao Q S, Lu W Z, Wang X C, et al, Novel zinc manganese oxide-based microwave dielectric ceramics for LTCC applications. *Ceram. Int.* 2015, 41(7): 9152-9156.
- [6] Cao Q S, Lu W Z, Zou Z Y, et al, Phase compositions and reaction models of zinc manganese oxides with different Zn/Mn ratios. *J. Alloy. Compd.* 2016, 661: 196-200.
- [7] Lei W, Lu W Z, Liu D, et al, Phase evolution and microwave dielectric properties of $(1-x)\text{ZnAl}_2\text{O}_4-x\text{Mg}_2\text{TiO}_4$ ceramics. *J. Am. Ceram. Soc.* 2009, 92(1): 105-109.
- [8] Kim J R, Kim D W, Cho I S, et al, Low temperature sintering and microwave dielectric properties of $\text{Ba}_3\text{Ti}_5\text{Nb}_6\text{O}_{28}$ with $\text{ZnO-B}_2\text{O}_3$ glass additions for LTCC applications. *J. Eur. Ceram. Soc.* 2007, 27(8): 3075-3079.
- [9] Kim J R, Kim D W, Jung H S, et al, Low-temperature sintering and microwave dielectric properties of $\text{Ba}_5\text{Nb}_4\text{O}_{15}$ with ZnB_2O_4 glass. *J. Eur. Ceram. Soc.* 2006, 26(10): 2105-2109.
- [10] Liang J, Lu W Z, Microwave dielectric properties of Li_2TiO_3 ceramics doped with $\text{ZnO-B}_2\text{O}_3$ frit. *J. Am. Ceram. Soc.* 2009, 92(4): 952-954.
- [11] Kim J S, Song M E, Joung M R, et al, Effect of B_2O_3 addition on the sintering temperature and microwave dielectric properties of Zn_2SiO_4 ceramics. *J. Eur. Ceram. Soc.* 2010, 30(2): 375-379.

- [12] Sayyadi-Shahraki A, Taheri-Nassaj E, Hassanzadeh-Tabrizi S A, et al, Low temperature cofirable $\text{Li}_2\text{Zn}_3\text{Ti}_4\text{O}_{12}$ microwave dielectric ceramic with Li_2O – ZnO – B_2O_3 glass additive. *J. Mater. Sci. - Mater. Electron.* 2014, 25(1): 355-360.
- [13] Lv X, Zheng Y, Zhou B, et al, Microwave dielectric properties of $\text{Li}_2\text{ZnTi}_3\text{O}_8$ ceramics doped with ZnO – SiO_2 – B_2O_3 glass. *Mater. Lett.* 2013, 91: 217-219.
- [14] Jantunen H, Rautioaho R, Uusimäki A, et al, Compositions of MgTiO_3 – CaTiO_3 ceramic with two borosilicate glasses for LTCC technology. *J. Eur. Ceram. Soc.* 2000, 20(14): 2331-2336.
- [15] Larson A C, Von Dreele R B. GSAS General Structure Analysis System, Report LAUR 86-748[J]. Los Alamos National Laboratory, Los Alamos, NM, 1986.
- [16] Toby B H, EXPGUI, a graphical user interface for GSAS, *J. Appl. Cryst.* 2001, 34(2): 210-213.
- [17] Hakki B W, Coleman P D, A dielectric resonator method of measuring inductive capacities in the millimeter range. *IEEE Trans. Microw. Theory Tech.* 1960, 8(4): 402-410.
- [18] Cao Q S, Microwave dielectric properties and LTCC characteristics of ZnO – MnO_2 based ceramic. Master thesis, Huazhong University of Science and Technology, 2016.
- [19] Reaney I M, Iddles D, Microwave dielectric ceramics for resonators and filters in mobile phone networks. *J. Am. Ceram. Soc.* 2006, 89(7): 2063-2072.
- [20] Tamura H, Microwave dielectric losses caused by lattice defects. *J. Eur. Ceram. Soc.* 2006, 26(10): 1775-1780.

- [21] Li J, Fang L, Luo H, et al. Li_4WO_5 : A temperature stable low-firing microwave dielectric ceramic with rock salt structure. *J. Eur. Ceram. Soc.* 2016, 36(1): 243-246.
- [22] Iddles D M, Bell A J, Moulson A J, Relationships between dopants, microstructure and the microwave dielectric properties of $\text{ZrO}_2\text{-TiO}_2\text{-SnO}_2$ ceramics. *J. Mater. Sci.* 1992, 27(23): 6303-6310.
- [23] Ullah B, Lei W, Cao Q S, et al, Structure and microwave dielectric behavior of A - Site - Doped $\text{Sr}_{(1-1.5x)}\text{Ce}_x\text{TiO}_3$ ceramics system. *J. Am. Ceram. Soc.* 2016, doi: 10.1111/jace.14341.
- [24] Xie H D, Chen C, Xi H H, et al, Synthesis, low temperature co-firing, and microwave dielectric properties of two ceramics BiM_2VO_6 (M=Cu, Ca). *Ceram. Int.* 2016, 42(1): 989-995.
- [25] Zang J, Li M, Sinclair D C, et al, Impedance spectroscopy of $(\text{Bi}_{1/2}\text{Na}_{1/2})\text{TiO}_3\text{-BaTiO}_3$ ceramics modified with $(\text{K}_{0.5}\text{Na}_{0.5})\text{NbO}_3$. *J. Am. Ceram. Soc.* 97 (2014) 1523-1529.
- [26] Rawal R, Feteira A, Flores A A, et al, Dielectric properties of the “twinned” 8H-hexagonal perovskite $\text{Ba}_8\text{Nb}_4\text{Ti}_3\text{O}_{24}$. *J. Am. Ceram. Soc.* 2006, 89(1): 336-339.

Table 1 Microwave dielectric properties of $(1-y)\text{Zn}(\text{Mn}_{0.2}\text{Al}_{0.8})_2\text{O}_4+y\text{TiO}_2$ ceramics with 5 wt.% ZB glass sintered at 950 °C for 3 h

y value	ϵ_r	$Q \times f$ (GHz)	τ_f (ppm/°C)
0.22	12.47	4251	-11.32
0.24	13.27	6443	-4.92
0.26	12.71	8027	1.02
0.28	13.70	7194	5.03

Fig. 1 XRD patterns of $\text{Zn}(\text{Mn}_{1-x}\text{Al}_x)_2\text{O}_4$ ($x=0.2-0.9$) ceramics at 1250 °C for 3 h: (a) cubic phase; (b) tetragonal phase; (c) $x=0.2$; (d) $x=0.4$; (e) $x=0.5$; (f) $x=0.6$; (g) $x=0.7$; (h) $x=0.8$; (i) $x=0.9$.

Fig. 2 The lattice parameters of $\text{Zn}(\text{Mn}_{1-x}\text{Al}_x)_2\text{O}_4$ solid solutions as a function of x value.

Fig. 3 SEM micrograph of $\text{Zn}(\text{Mn}_{1-x}\text{Al}_x)_2\text{O}_4$ ceramics sintered at 1250 °C: (a) $x=0.4$, (b) $x=0.5$, (c) $x=0.6$, (d) $x=0.7$, (e) $x=0.8$, (f) $x=0.9$.

Fig. 4 Dielectric constant (ϵ_r) of the $\text{Zn}(\text{Mn}_{1-x}\text{Al}_x)_2\text{O}_4$ ceramics as a function of x value.

Fig. 5 The $Q \times f$ (a), τ_f (b), and relative density (c) of the $\text{Zn}(\text{Mn}_{1-x}\text{Al}_x)_2\text{O}_4$ ceramics as a function of x value.

Fig. 6 Arrhenius fitting plot from the temperature dependence of the bulk conductivity

for $\text{Zn}(\text{Mn}_{1-x}\text{Al}_x)_2\text{O}_4$ ($0.2 \leq x \leq 0.9$) ceramics.

